Contribution from the Department of Chemistry,
Northwestern University, Evanston, Illinois 60201

Variable-Temperature Raman and Infrared Spectra of the Copper Acetate Dimer $Cu_2(O_2CCH_3)_4(H_2O)_2$ and Its Derivatives

Y. MATHEY,*[1a] D. R. GREIG,[1b] and D. F. SHRIVER*

Received March 2, 1982

Variable-temperature Raman spectra have been obtained on normal isotopic $Cu_2(O_2CCH_3)_4(H_2O)_2$ and its various ^2H, ^{18}O, and ^{65}Cu isotopomers. These data, along with Raman spectroscopic data on the derivatives $Cu_2(O_2CCH_3)_4L_2$ where L = pyridine (py) or 0.5 pyrazine ($(pyz)_{1/2}$), reveal that a temperature-dependent feature around 300 cm^{-1} in the aquo complex is a CuO stretch for the axial water ligands and not an electronic Raman transition. These Raman data, supplemented with new infrared spectra, were employed to make some detailed vibrational assignments.

The tetrakis(acetato)dimetal complexes I range from

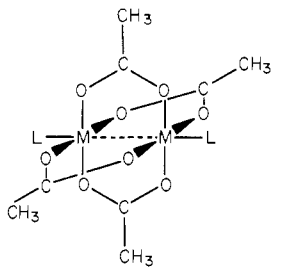

I

strongly metal–metal bonded species such as $Mo_2(O_2CCH_3)_4$, which contains a formal quadrupole Mo≡Mo bond, to the weakly interacting metal centers such as copper in the copper acetate dimer.[2,3] Raman spectroscopy affords a promising tool for the study of these extremes in metal–metal interaction and for the delineation of the role of the acetato bridges.[4] The infrared and Raman spectra have been determined in some detail for dimolybdenum tetraacetate and related compounds.[5-7] In agreement with the presence of a quadrupole bond, the Mo–Mo stretch in this compound is quite high and the metal isotope effects on the stretching frequency indicate that the acetato bridges contribute little to the Mo–Mo restoring force.[5]

The present vibrational spectroscopic study of the copper acetate dimer was undertaken to explore the opposite extreme of metal–metal bonding and to determine if any manifestations can be found in the vibrational spectra for the equilibrium between singlet and triplet electronic states. The electronic structure of the copper acetate dimer, which has been the topic of many experimental and theoretical investigations,[2,3,8] is well documented; however, the vibrational spectroscopy of this molecule is largely unsettled. Temperature-dependent magnetic susceptibility and ESR data indicate the presence of a singlet ground state for this molecule, which is separated from a triplet excited state by $-2J \simeq 300$ cm^{-1}. Owing to this small energy separation, there is appreciable thermal population of the triplet state at ambient temperature. The single–triplet energy separation, $-2J$, is approximately the same for the dihydrate and the anhydrous material, where the oxygen atoms from neighboring molecules may fill the axial sites as found with anhydrous copper propionate and butyrate.[2] The value of $-2J$ is significantly increased when axial water ligands are replaced by nitrogenous ligands such as pyridine (py)[8] or pyrazine ($(pyz)_{1/2}$).[9]

Experimental Section

Infrared spectra were collected on a Nicolet 7199 Fourier transform spectrometer. The Raman data were determined with a Spex 1401 double monochromator, with use of argon ion and krypton ion laser excitation, back-scattering sampling optics of our own design, an RCA C31034 photomultiplier operating in the photon-counting mode, and digital acquisition. Most of the data were logged onto digital magnetic tape and processed off-line at the Northwestern University Computing Center. For the highest possible accuracy of the isotope shifts, these particular data were collected by a two-channel technique in which the spectrometer drive, data acquisition, and data processing were all performed under the control of a Nova 2 minicomputer (Figure 1). This experimental arrangement is advantageous for the determination of small isotope shifts because Raman data are collected on both samples at the same wavenumber position of the monochromator; the wavenumber position is then incremented and data are again collected for both samples. In this way the relative wavenumbers of closely spaced bands are determined much more accurately than by using the conventional technique of separate scans for each sample. Low-temperature Raman spectra were collected on spinning samples cooled by boil-off from liquid nitrogen or samples attached to the tip of a Displex closed-cycle helium refrigerator.

Syntheses of hydrated copper acetate and of some isotopically substituted isomers, $^{nat}Cu_2(O_2CCH_3)_4(H_2O)_2$, $^{65}Cu_2(O_2CCH_3)_4(H_2O)_2$, and $^{nat}Cu_2(O_2CCD_3)_4(H_2O)_2$, were carried out by the reaction of appropriate amounts of copper(II) oxide, glacial acetic acid, and water.[11,12] D_2O and $H_2{}^{18}O$ hydrates were prepared by rehydration of the anhydrous dimeric compound $Cu_2(O_2CCH_3)_4$. Anhydrous $Cu_2(O_2CCH_3)_4$ was obtained by gentle heating (ca. 130 °C) of ground $Cu_2nO_2CCH_3)_4(H_2O)_2$ powder under dynamic vacuum.

All products were checked by infrared spectroscopy using the high-frequency isotope-sensitive modes as internal probes. Crystals of $Cu_2(O_2CCH_3)_4(py)_2$ were obtained by the addition of pyridine to a solution of copper acetate in acetonitrile, followed by slow evaporation. A crystalline sample of $Cu_2(O_2CCH_3)_4(pyz)$ was prepared by diffusion of an aqueous solution of pyrazine into a saturated aqueous solution of $Cu_2(O_2CCH_3)_4(H_2O)_2$.[10]

Results

Infrared and Raman spectra for several isotopic forms of $Cu_2(O_2CCH_3)_4(H_2O)_2$ are presented in Tables I and II. Table

(1) (a) Permanent address: Universite de Paris-Sud, Laboratoire Physicochemie Minerale, 91405 Orsay, France. (b) Permanent address: Varian Associates, Palo Alto, CA 94303.
(2) Catterick, J.; Thornton, P. *Adv. Inorg. Chem. Radiochem.* **1977**, *20*, 291-362.
(3) Doedens, R. J. *Prog. Inorg. Chem.* **1976**, *21*, 209–231.
(4) Shriver, D. F.; Cooper, C. B., III. *Adv. Infrared Raman Spectrosc.* **1980**, *6*, 127.
(5) Hutchinson, B.; Morgan, J.; Cooper, C. B., III; Mathey, Y.; Shriver, D. F. *Inorg. Chem.* **1979**, *18*, 2048–2049.
(6) Bratton, W.; Cotton, F. A.; Debeau, M.; Walton, R. A. *J. Coord. Chem.* **1971**, *1*, 121.
(7) Ketteringham, A. P.; Oldham, C.; Peacock, C. J. *J. Chem. Soc., Dalton Trans.* **1976**, 1640.
(8) Jotham, R. W.; Kettle, S. F. A.; Marks, J. A. *J. Chem. Soc. A* **1972**, 428.
(9) Valentine, J. S.; Silverstein, A. J.; Soos, Z. G. *J. Am. Chem. Soc.* **1974**, *96*, 97.
(10) Kawamori, A. *J. Chem. Phys.* **1971**, *55*, 1336.
(11) Kirchner, S. J.; Schubert, S. A.; Mounts, R. D.; Fernando, Q. *Inorg. Chim. Acta* **1978**, *27*, L80.
(12) Heyns, A. M. *J. Mol. Struct.* **1972**, *11*, 93.

0020-1669/82/1321-3409$01.25/0 © 1982 American Chemical Society

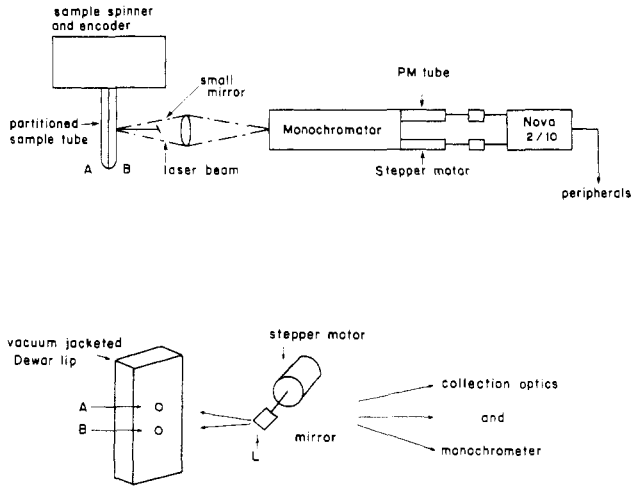

Figure 1. Schematic representation of the two-channel apparatus for Raman back-scattering: (top) spinning samples in a partitioned tube; (bottom) samples on a Dewar tip for low-temperature spectroscopy.

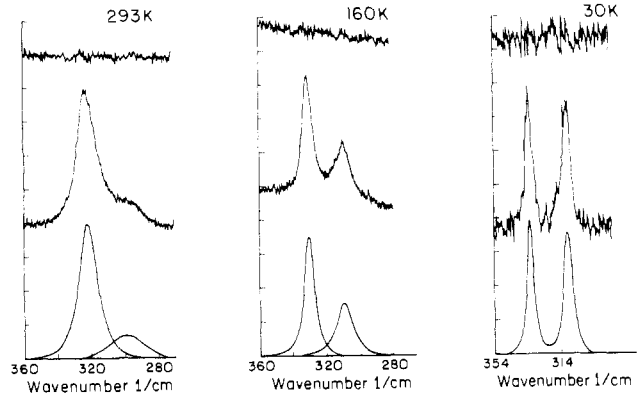

Figure 2. Temperature dependence of composite and difference spectra for $Cu_2(O_2CCH_3)_4(H_2O)_2$ in the 320-cm^{-1} region (λ_0 = 514.5 nm). In each frame the middle spectrum is raw data, the lower is the two-band fit, and the upper is the difference between observed and fitted spectra.

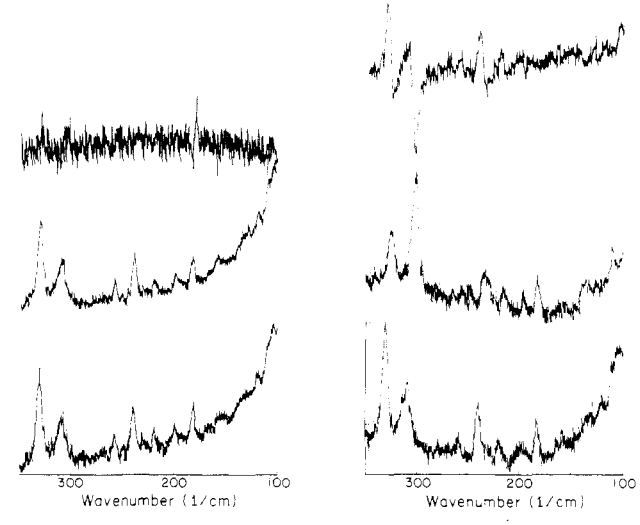

Figure 3. Representative difference spectra for isotopic variants of $Cu(O_2CCH_3)_4)(H_2O)_2$: (left) ^{65}Cu complex – ^{nat}Cu complex; (right) CH_3COO-containing complex – CD_3COO-containing complex.

III summarizes the results obtained in the low-frequency range (700–50 cm^{-1}) for the anhydrous copper acetate and for $Cu_2(O_2CCH_3)_4L_2$ with L = py or $(pyz)_{1/2}$. Where comparisons can be made with published infrared data on the normal isotopic molecule, the agreement is generally good.[13] Inter-

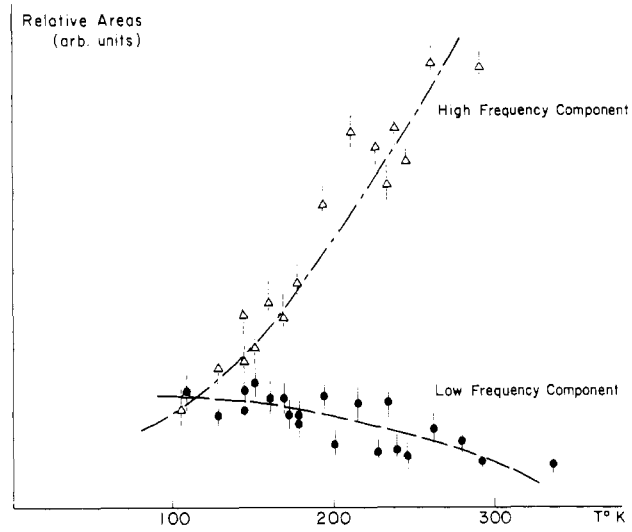

Figure 4. Relative areas of the two fitted components in the 300-cm^{-1} region vs. temperature.

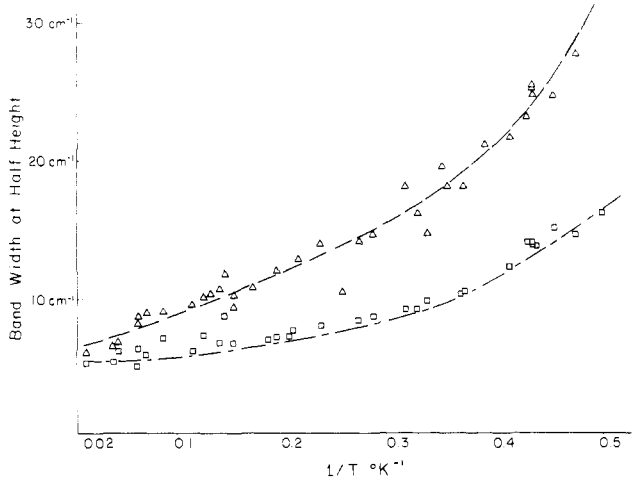

Figure 5. Half-width at half-height of the two fitted components in the 300-cm^{-1} region vs. triplet to singlet ratio, n_T/n_S.

esting variations of intensity with temperature were found in the 300-cm^{-1} region (Table II), and a sampling of these spectra is depicted in Figure 2. Some representative two-channel Raman spectra are displayed in Figure 3 for the copper isotopomers.

Discussion

The most striking influence of temperature on the Raman spectra was observed in the 300-cm^{-1} region, which is very close to the singlet–triplet energy separation. Subsequent to the collection of the present data, Gudel reported the direct observation of this electronic transition in the inelastic-neutron-scattering spectrum,[13] and at the time of our experiments we seriously considered the possibility that we were observing the singlet–triplet transition via electronic Raman scattering. According to the selection rules for electronic Raman scattering, the single–triplet transition is forbidden, but selection rules might be relaxed by spin–orbit coupling. Therefore experiments were designed to determine the origin of these Raman bands. Temperature-dependent Raman data in the 300-cm^{-1} region were deconvoluted into two bands by means of a digital least-squares fitting procedure, and relative areas, normalized to the 254-cm^{-1} band, were plotted against temperature (Figure 4). Contrary to initial impressions from the

(13) Gudel, H. U.; Stebler, A.; Furrer, A. *Inorg. Chem.* **1979**, *18*, 1021–1023.

Table I. Room-Temperature Infrared and Raman Spectra (2000–50 cm^{-1}) for $Cu_2(O_2CCH_3)_4(H_2O)_2$[a]

	$^{nat}Cu_2(O_2CCH_3)_4(H_2O)_2$		$^{65}Cu_2(O_2CCH_3)_4(H_2O)_2$		$^{nat}Cu_2(O_2CCH_3)_4(H_2{}^{18}O)_2$		$^{nat}Cu_2(O_2CCH_3)_4(D_2O)_2$		$^{nat}Cu_2(O_2CCD_3)_4(H_2O)_2$	
	IR	Raman	IR	Raman	IR	Raman	IR	Raman	IR	Raman
$\nu_{asym}(COO)$	1605 vs		1618 vs		1604 vs				1600 vs	
			1597 vs							
$\delta_{asym}(CH_3)$	1460 sh	1450 w	1442 vs	1436 w	1442 vs			1438 vw	1450 vs	
			1421 vs	1418 w	1421 vs					
$\nu_{sym}(COO)$	1425 m									1421.5 w
	1410 sh									
$\delta_{sym}(CH_3)$	1356 m		1357 m	1358 w	1357 m					
...					1266 w					
$\delta(DOD)$							1212 m			
...					1104 w		1120 w			
$\delta_{asym}(CD_3)$									1093 w	1093 w
$\rho(CH_3)$	1053 m		1054 m		1047 m		1051 m		1045 sh	
	1049 sh		1033 m		1033 m		1032 m			
	1032 m									
$\delta_{sym}(CD_3)$									1032 m	1026 w
...							970 vw			
$\nu(C-CH_3)$	945 vw	948 s		948.5 s		951 s	945 vw	949 m	927 s	
		938 m		940 m			890 vw	940 w		
		899 w		900 w				899 vw		
$\rho(CD_3)$									893 m	901 m
										892 m
$\nu(C-CD_3)$									851 m	
...							845 vw			
...	795 vw						770 vw			
$\delta_{sym}(COO)$	690 vs	702 m	695 vs	704 m	695 vs	704.5 m	689 s	702.5 m	663 vs	676 m
		683 w		685 w				684.5 w		
$\rho(COO)$	625 s	640 vw	631 s		631 s		627 s			
$\rho(H_2O)$	560 w		561 m		526 m				546 s	
	525 w		526 m						519 w	
$\rho(COO)$	460 vw						465 w		478 sh	
$\rho(D_2O)$							425 vw			
$\nu(Cu-O)$	376.5 sh						374 s		366 s	
	373 s									
$\nu(Cu-O)$	330 s	323 s		323 s		321.5 s	330 m	322 s	325 s	313 s
$\nu(Cu-O_w)$		302 sh		302 sh		299 sh			300 sh	298 m
...								288 vw		
$\delta(Cu-Cu-O_w)$	272 vs	254 m		254 m		254 w	265 w	253.5 m	252 s	250 w
	253 m									
...								244 vw		
$\delta(O-Cu-O)$	233 m	234 s		234 m		233 m	230 sh	229 w	235 sh	227 w
		223 w		226 sh		226 sh				222 w
...				215 w		215 w		214.5 w		211 w
$\delta(O-Cu-O)$	184 m	181 m		179 m		180 m		179 m		181 w
$\delta(Cu-Cu-O)$ ring def		158 w		157.5 m		156 vw		157.5 m		156 w
...		127 w		128 w		125 w				132 w
$\delta(Cu-Cu-O_w)$	114 w									
...		107 w		107 w		107 m		117 vw		118 w
...								105 w		108 w
...		92.5 w			93 w		90 m			94 w
$\delta(Cu-Cu-O)$ ring def		83.5 w			82 w					
...	73 m	71 w		72 w		72 w				

[a] O_w indicates an oxygen atom from water ligands.

raw data, the low-frequency band around 300 cm^{-1} gains relatively little intensity at low temperature.

Strong evidence against the assignment of the 300-cm^{-1} feature to the singlet–triplet transition was obtained for compounds in which the axial H_2O ligands have been replaced by other ligands. As shown in Table II, axial D_2O or $H_2{}^{18}O$ ligation has a much larger effect on the 300-cm^{-1} feature than would be expected if the transition were electronic in origin. Furthermore the shifts in the band are of the right magnitude in the case of the ^{18}O species for the assignment of this feature to a Cu–O vibrational mode. The value of $-2J$ for $Cu_2(O_2CCH_3)_4(pyz)$ is 325 cm^{-1}, and therefore the Raman spectrum of this compound was carefully examined in this region, but no new Raman bands attributable to a singlet–triplet transition were observed; instead new bands are found near 260 cm^{-1}, which are reasonably assigned as Cu–N stretching modes. In summary, the spectra on these copper acetate derivatives demonstrate that the 300-cm^{-1} band should be assigned to a Cu–O stretch for the axial water molecules, and not to an electronic transition. The strong temperature-dependent damping of this band (Figure 5) probably originates from the extensive intermolecular hydrogen-bonded network of these water ligands, which is expected to be highly anharmonic. Clearly, the selection rules prohibiting the spin-flip transition are not relaxed sufficiently to permit observation of this transition in the Raman spectrum. Inelastic neutron scattering, which is not controlled by strong selection rules, is at present the only technique for the direct observation of this transition.

The Cu–Cu stretch is of interest for comparison with acetate-bridged metal–metal bonded compounds; also this frequency is of some importance to the interpretation of the temperature-dependent magnetic properties of the copper acetate dimers. Estimates around 100 cm^{-1} for this frequency

Table II. Raman Spectra and Temperature Effect in the Low-Frequency Range (350–50 cm^{-1}) for Several Isotopomers of Copper Acetate Dimer[a]

	$^{nat}Cu_2(O_2CCH_3)_4(H_2O)_2$		$^{65}Cu_2(O_2CCH_3)_4(H_2O)_2$		$^{nat}Cu_2(O_2CCH_3)_4(H_2{}^{18}O)_2$		$^{nat}Cu_2(O_2CCH_3)_4(D_2O)_2$		$^{nat}Cu_2(O_2CCD_3)_4(H_2O)_2$	
	300 K	150 K	300 K	150 K	300 K	160 K	300 K	180 K	300 K	120 K
ν(Cu–O)	323 s	331 s	323 s	331 s	321.5 s	324.5 s	332 s	327.5 s	313 s	327 m
ν(Cu–O_w)	302 sh	308 m	302 sh	308 m	299 sh	300.5 m		303 vw	298 sh	304 s
				307 m						
...							288 vw			
δ(Cu–Cu–O_w)	254 m	258 m	254 w	258 m	254 w	257 m	253.5 m	254 m	250 w	256 w
										250 w
...							244 vw			
δ(O–Cu–O)	234 s	239.5 s	234 m	239.5 s	233 m	237.5 m		238 s		235.5 m
										233 m
...	223 w	219 vw	226 sh	219.5 m	226 sh		229 vw	227 w	227 w	
		218 vw	215 m	217.5 w	215 w		214.5 w	216 m	222 w	
									211 w	215.5 w
...		198 w		199.5 w		190 w		195 w		196.5 w
δ(O–Cu–O)	181 m	183.5 m	179 m	181 m	180 m	179 m	179 m	178 m	181 w	182.5 m
		182 m								
δ(Cu–Cu–O) ring def	158 w	158 w	157.5 m	158.5 vw	156 vw	157 vw	157.5 m	157 m	156 w	157.5 w
δ(Cu–Cu–O_w)	127 w	125 vw	128 w	124.5 vw	125 w	133 vw	117 vw	116.5 vw	118 w	124.5 w
	107 w	118 vw	107 w	109 m	107 m	108 w	105 w		108 w	110.5 m
		109 vw								
...				104.5 m						
δ(Cu–Cu–O) ring def	92.5 w	94 m	93 m		90 m			92.5 m	94 w	94 s
...	83.5 w		82 w							
...	71 w	71.5 w	72 w		72 w					

[a] O_w indicates an oxygen atom from water ligands.

Table III. Room-Temperature Infrared and Raman Spectra (780–50 cm^{-1}) for the Copper Acetate Dimer and Some of Its Derivatives[a]

	$Cu_2(O_2CCH_3)_4(H_2O)_2$		$Cu_2(O_2CCH_3)_4$ (anhyd)		$Cu_2(O_2CCH_3)_4(py)_2$		$(Cu_2(O_2)CCH_3)_4(pyz)$	
	IR	Raman	IR	Raman	IR	Raman	IR	Raman
δ_{sym}(COO) and δ(C–H)-(heterocyclic ligand)(·)[b]		702 m		702 s		700 s		
	690 vs		691 vs					
		683 w		685 w		680(·)m[b]	686.5 sh	695 vs
							679.5(·)s	
ρ(COO) and δ_{ring}-(heterocyclic ligand)(·)		640 vw				645 vs	640 sh	645 w
	625 s		626 vs			630(·)s	631(·)m	
$\rho(H_2O)$	560 w							
	525 w							
ρ(COD) and δ_{ring}-(heterocyclic ligand)(·)	460 vw		465 w					
					419(·)s	420(·)w	417(·)m	
ν(Cu–O)	376.5 sh		388 s	365 w	353 vs		357 s	311 vs
	373 s		342 s					
ν(Cu–O)	330 s	323 s		315 vs		303 vs		311 vs
ν(Cu–O_w)		302 sh						
δ(Cu–Cu–O_w)	272 vs							
ν(Cu–N)(·)	253 m	254 m			266(·)vs	252(·)vw	256(·)m	258(·)w
δ(O–Cu–O)	233 m	234 s	235 m	241 m	230 w	234 m	234 m	236 m
		223 w		232 w		224 w		213.5 m
				226 m		212 m		
				217 w				
δ(O–Cu–O)	184 m	181 m	180 m		185 m	189 vw	192 m	
δ(Cu–Cu–O) ring def		158 w		153 m		161 w	162 m	158 w
δ(Cu–Cu–O_w)	114 w	127 w						
...		107 w	105 w	108 w				109 s
δ(Cu–Cu–O) ring def		92.5 w		93 w				92 s
...		83.5 w						
...	73 m	71 w		76 w			74 m	
...					53 vs			

[a] O_w indicates an oxygen atom from water ligands. [b] (·) identifies modes associated with deformation of the metal carboxylate ring.

have appeared at least twice in the literature,[2] but it has not been observed directly, so two-channel Raman data were collected on $^{65}Cu_2(O_2CCH_3)_4(H_2O)_2$ and its analogue of natural isotopic composition. The largest copper isotopic shift, ca. 1.8 cm^{-1}, is observed in a band around 183 cm^{-1} in the normal isotopic molecule. This is 64% of the calculated shift for a diatomic Cu_2 species and indicates a large amplitude for Cu in this normal mode. This band is at a very high frequency for a Cu–Cu stretch, because unsupported M–M stretching frequencies for first-row transition metal compounds having single M–M bonds are found around 160 cm^{-1}.[4] Even though a large component of Cu–Cu motion is indicated in the eigenvector, we believe that the best description of the 183-cm^{-1} band is a CuO_4 symmetric deformation because the potential energy should be mainly localized in the Cu–O bond rather than the stretch of a very weak or possibly nonexistent Cu–Cu bond.

The known vibrational spectrum of the free acetate ion and our observed isotope effects permit convincing assignment of high-frequency modes (Tables I and III). The low-frequency

region is more complex; so despite the variety of isotopic spectral shifts collected here, some of the low-frequency Raman features remain unassigned.

Acknowledgment. This research was supported by a grant from the Petroleum Research Fund, administered by the American Chemical Society. Y.M. was the recipient of a NATO Postdoctoral Fellowship.

Registry No. $Cu_2(O_2CCH_3)_4(H_2O)_2$, 15523-07-6; ^{65}Cu, 14119-06-3; ^{18}O, 14797-71-8; D_2, 7782-39-0; $Cu_2(O_2CCH_3)_4(py)_2$, 15227-71-1; $Cu_2(O_2CCH_3)_4(pyz)$, 51798-89-1.

Contribution from the Laboratoire de Chimie de Coordination Bioorganique (LA 255), Centre d'Orsay de l'Université Paris-Sud, 91405 Orsay, France, and Laboratoire de Chimie Analytique, Centre d'Etudes Pharmaceutique, Université Paris-Sud, 92290 Chatenay-Malabry, France

Structural Studies of Metalloporphyrins. 7.[1] ^{1}H NMR and Electrochemical Investigation of the (*meso*-5,10,15,20-Tetraarylporphine)cobalt(III) Complexes XCo^{III}(TPP-*p*-R)[2]

J. HUET,* A. GAUDEMER, C. BOUCLY-GOESTER, and P. BOUCLY

Received October 22, 1980

^{1}H NMR spectra of five-coordinate cobalt(III) *meso*-5,10,15,20-tetraarylporphines XCo^{III}(TPP-*p*-R) (X = I, Br, Cl, PF_6, ClO_4; R = H, Cl, CH_3, OCH_3) display abnormally broad line widths. The magnitude of this line broadening varies with X and R and generally increases with temperature. Analysis of the data obtained at various temperatures suggests that this phenomenon is due in part to the presence of a small amount of the π-cationic species XCo^{III}(TPP-*p*-R)$^{+\cdot}$, which is formed by the following disproportionation reaction: $2XCo^{III}(TPP\text{-}p\text{-}R) \rightleftarrows Co^{II}(TPP\text{-}p\text{-}R) + XCo^{III}(TPP\text{-}p\text{-}R)^{+\cdot} + X^-$. Electrochemical data obtained in CH_2Cl_2 solution fully support this assumption. A second, but less important, source of the line broadening appears to be the self-exchange reaction between cobalt(II) and cobalt(III) porphyrins, which results in an exchange of ligand X and of protonated sites.

The magnetic properties of cobalt(III) complexes such as vitamin B_{12} and various model compounds (cobaloximes, porphyrins) have been the subject of many studies leading to contradictory results and interpretations.[3] Although most cobalt(III) complexes are diamagnetic because of their d^6 low-spin configuration ($S = 0$), some of them having a high-spin configuration are paramagnetic: apart from $Co^{III}F_6^{3-}$ ($S = 2$)[4] and complexes of the structure $Co^{III}(P(C_2H_5)_3)X_3$ (X = Cl, Br) ($S = 1$)[5] some macrocyclic cobalt(III) complexes exhibit a paramagnetism[6] the extent of which varies with the macrocyclic ligand and increases with temperature due to an equilibrium between low-spin and high-spin configurations.[7-9] According to some authors,[7] cobalt(III) porphyrins should be diamagnetic due to the strong ligand field created by the macrocycle. The weak magnetic susceptibility observed for $ClCo^{III}(HP)(H_2O)$ in the solid state could arise from cobalt(II) impurities or from the temperature-independent paramagnetism (TIP).[10]

^{1}H NMR spectroscopy is very sensitive to the magnetic characteristics of compounds. Various features of the species—chemical shifts,[8] line widths,[11] H–H and H–Co coupling constants[11,12]—have been repeatedly used to study the properties of cobalt(III) complexes and also to obtain structural evidence for the existence of π-cationic species derived from metalloporphyrins.[13]

Two groups of investigators[14,15] recently observed that, in solution in a noncoordinating solvent, the cobalt(III) porphyrins $ClCo^{III}$(TPP),[14] $[Co^{III}(TPP)(H_2O)_2]ClO_4$, $[Co^{III}(OEP)(H_2O)_2]ClO_4$, and $[Co^{III}(OEP)(THF)_2]ClO_4$[15] exhibit abnormally broad lines in their ^{1}H NMR spectra, suggesting a paramagnetic character for these compounds. On the basis of variable-temperature measurements using Evans' method,[16] it was concluded that $ClCo^{III}$(TPP) showed a paramagnetism that increased with temperature.[14]

In the present work, we report the results of an ^{1}H NMR study of various complexes XCo^{III}(TPP-*p*-R) shown in Figure 1, which indicates that the line broadening has multiple origins and that the paramagnetism of these compounds probably does not arise from an equilibrium between low-spin and high-spin forms. Electrochemical data are also presented which, together with the NMR study, lead to other possible explanations for this paramagnetism.

Results and Discussion

I. ^{1}H NMR Spectra of Complexes XCo^{III}(TPP-*p*-R). In 0.02–0.03 M solution in $CDCl_3$, most of the complexes shown in Figure 1, except those with X = I, show abnormally broad NMR signals. The extent of broadening varies with the nature of X and R and with temperature.

* To whom correspondence should addressed at the Laboratoire de Chimie de Coordination Bioorganique.

(1) Part 6: J. Huet and A. Gaudemer, *Org. Magn. Reson.*, **15**, 347 (1981).
(2) Abbreviations used in this work for porphyrin complexes: HP, hematoporphyrin; TPP, *meso*-5,10,15,20-tetraphenylporphine; TPP-*p*-R, *meso*-5,10,15,20-tetraarylporphine; OEP, octaethylporphine; H_β refers to the proton of the pyrrole ring.
(3) For a detailed review on the magnetic properties of vitamin B_{12} see S. C. Agarwal, *Bull. Soc. Chim. Fr.*, I-100 (1979).
(4) F. A. Cotton and G. Wilkinson, "Advanced Inorganic Chemistry", 2nd ed., Interscience, New York, 1966, p 671.
(5) K. A. Jensen, B. Nygaard, and C. Th. Pedersen, *Acta Chem. Scand.*, **17**, 1126 (1963).
(6) R. Williams, E. Billig, J. H. Waters, and H. B. Gray, *J. Am. Chem. Soc.*, **88**, 43 (1966).
(7) M. Gerloch, B. M. Higson, and E. D. McKenzie, *J. Chem. Soc., Chem. Commun.*, 1149 (1971).
(8) V. L. Goedken and Shie-Ming Peng, *J. Chem. Soc., Chem. Commun.*, 258 (1975).
(9) M. Lundeen, R. L. Firor, and K. Seff, *Inorg. Chem.*, **17**, 701 (1978).
(10) W. P. Hambright, A. N. Thorpe, and C. C. Alexander, *J. Inorg. Nucl. Chem.*, **30**, 3139 (1968).
(11) J. L. Sudmeier and G. L. Blackmer, *J. Am. Chem. Soc.*, **92**, 5238 (1970).
(12) J. L. Sudmeier, A. J. Senzel, and G. L. Blackmer, *Inorg. Chem.*, **10**, 90 (1971).
(13) J. K. M. Sanders and I. Baxter, *Tetrahedron Lett.*, 4543 (1974).
(14) K. Yamamoto, J. Uzawa, and T. Chijimatsu, *Chem. Lett.*, 89 (1979).
(15) H. Sugimoto, M. Nagano, Z. Yoshida, and H. Ogoshi, *Chem. Lett.*, 521 (1980).
(16) D. F. Evans, *J. Chem. Soc.*, 2003 (1959).

0020-1669/82/1321-3413$01.25/0 © 1982 American Chemical Society